Pergamon

Tetrahedron Vol. 51, No. 11, pp. 3149-3158, 1995

0040-4020/95 $9.50+0.00

0040-4020(95)00088-7

Structure and Enantiomerization of Helically Twisted Lactone–Bridged Biaryls: a Theoretical Study[1]

Gerhard Bringmann*, Holger Busse, Ulrich Dauer, Stefan Güssregen and Martin Stahl
Institut für Organische Chemie, Universität Würzburg, Am Hubland, 97074 Würzburg, Germany

Abstract: Structures of benzo[b]naphtho[1,2–d]pyranones, helically twisted bridged biaryl precursors in stereoselective biaryl synthesis, were calculated by semiempirical (AM1, PM3) methods and compared with those obtained by *ab initio* calculations (MP2/6-31G*//RHF/3-21G) for one of the compounds. The structural parameters match excellently with those previously obtained through X–ray structure analyses. For the helimerization process of the title compounds, the activation barriers were determined by locating the corresponding transition structures.

INTRODUCTION

The directed synthesis of axially chiral biaryl systems[2] requires the regioselective coupling of two aromatic ring systems *and* the stereoselective introduction of chirality at the newly created stereogenic axis. We have recently developed a procedure in which these two formal goals of stereoselective biaryl synthesis are solved independently, by two separate steps.[3–5] First the *CC*–bond formation is performed by intramolecular aryl aryl coupling of the two ester–type prefixed aromatic systems to give lactone–bridged biaryls in high chemical yields and reliable regioselectivities.[6,7] In a second step, using chiral metalated nucleophiles, these more or less rapidly helimerizing and thus configuratively unstable bridged biaryls like **1** are opened such that only one of the two possible atropisomeric, configuratively stable cleavage products **2** is formed in high selectivities (Scheme 1).[3–5,8] For a further optimization of the procedure and its extension also to other types of nucleophiles, an

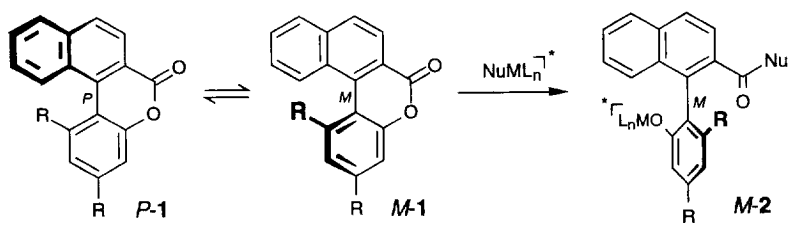

1	a	b	c	d	e	f
R	H	OMe	Me	Et	*i*Pr	*t*Bu

Scheme 1. The atropisomer–selective ring opening reaction of benzo[b]naphtho[1,2–d]pyranones; labile stereogenic elements (centers or axes) are denoted by '○' stable ones by'∗'.

elucidation of the mechanism of this unprecedented principle of stereocontrol would be highly desirable. In this paper, we report on the calculation of the helically twisted ground state structures of a complete series of lactones **1**, with variable steric hindrance next to the biaryl axis, ranging from R = H to *t*Bu, by semiempirical and (in one representative case) *ab initio* methods. The results show a high degree of agreement with structural parameters gained experimentally through X–ray structure analyses. Furthermore, the transition structures and thus the barriers for the interconversion of the two helimeric enantiomers *P*–**1** and *M*–**1** were calculated.

COMPUTATIONAL METHODS

Semiempirical calculations (AM1[9] and PM3[10]) were performed on Silicon Graphics IRIS 4D/310 GTX and INDIGO (R4000) workstations using the VAMP 4.5[11] program. Input geometries were taken from random search calculations within the TRIPOS force field as implemented in SYBYL.[12] Ground structures were minimized until a gradient norm of less than 0.01 mdyn/Å was achieved; transition structures were optimized using the NS01A algorithm by Powell[13] with the same gradient specifications. Geometries of all stationary points were subjected to force calculations in order to obtain thermodynamic data for zero point correction of the activation barriers. The *ab initio* calculations were carried out on a CRAY Y–MP 4/464 by means of the Gaussian 92[14] program. Geometries of ground and transition structures were determined on the RHF/3–21G level. Zero point corrected activation barriers were obtained by means of frequency calculations at the same level. Energies were calculated at the MP2/6–31G* level as well. Transition states were located using the TS algorithm by Baker.[15]

RESULTS AND DISCUSSION

Ground structures

Initial force field calculations (TRIPOS) suggest that the central lactone ring occurs in two distinct conformations, a twist boat and a chair form (and their enantiomers). By contrast, only the two enantiomeric twist boat conformations proved to be minimum structures according to the semiempirical calculations. These minimum structures were compared with those obtained from X–ray structure analyses.[6,16,17]

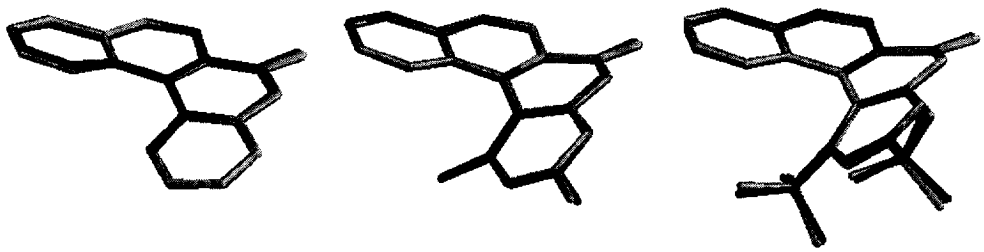

Fig. 1. Superimposed experimental (X–ray structures, dark) and calculated (PM3, bright) structures of **1a**,**1c**, and **1f** (*P*–helimer, respectively), selected representatives of the biaryl lactones

As visualized in Figure 1, exemplarily for **1a**, **1c**, and **1f** (representing weak, medium, and strong steric hindrance, resp.), the agreement between calculated and experimental geometries is excellent, the structures match nearly perfectly. This is further underlined by the RMS values as a measure of the small structural deviations (Table 1). From these values, no distinct qualitative difference between the AM1 and PM3 parametrizations can be deduced.

As mentioned, the lactones **1a–f** occur as two chiral enantiomeric rotational isomers with respect to the biaryl axis, helically twisted minimum structures. Their molecular distortion concerns the whole molecule,

Table 1. Ground states of the lactones. Heats of formation (kcal/mol), dihedral angles (deg.), inner spiral loop ($\Sigma_{\alpha\beta\gamma}$); RMS values (Å) refer to the X–ray structures and were calculated for ring atoms only.

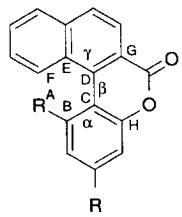

Cpd.	Method	ΔH_f	Selected Dihedral Angles					RMS
			α ABCD	β BCDE	γ CDEF	$\Sigma_{\alpha\beta\gamma}$	HCDG	
1a	AM1	7.32	4.4	20.8	17.4	42.6	16.9	0.095
	PM3	-4.30	1.2	17.5	14.1	32.8	13.9	0.087
	exp.[a]	–	–	26.0	15.7	–	5.2	–
1b	AM1	-63.70	8.6	28.7	16.2	53.5	22.3	0.066
	PM3	-73.51	13.1	32.9	16.6	62.6	25.1	0.075
	exp.[b]	–	6.0	32.2	17.2	55.4	21.8	–
1c	AM1	-2.25	14.4	31.4	16.0	61.8	25.0	0.060
	PM3	-16.01	14.6	33.7	16.2	64.5	26.2	0.052
	exp.[b]	–	12.4	34.1	15.0	61.5	25.7	–
1d	AM1	-12.19	16.2	32.3	14.8	63.3	26.0	0.061
	PM3	-24.61	17.1	34.9	15.0	67.0	27.3	0.063
	exp.[b]	–	14.5	34.0	14.4	62.9	25.2	–
1e	AM1	-19.63	18.3	34.6	14.7	67.6	27.2	0.051
	PM3	-34.15	17.6	35.2	13.6	66.4	27.4	0.049
	exp.[b]	–	18.1	34.1	14.4	66.6	25.0	–
1f	AM1	-14.43	31.6	38.3	10.4	80.3	31.4	0.046
	PM3	-35.70	25.8	41.3	9.8	76.9	32.4	0.067
	exp.[c]	–	33.7	36.0	8.5	78.2	29.6	–

[a] see ref. 16, [b] see ref. 6, [c] see ref. 17

which adopts, according to the steric demand of the *ortho* substituents R, a more or less severely distorted screw–like helix. A good measure for this molecular distortion is the sum of the three dihedral angles α, β and γ (see Table 1), defined as the "inner spiral loop".[6,18]

In terms of molecular strain, the ground state is characterized by two effects. The first one is based on the fact that the two aryl systems are not coplanar to each other (angle β), resulting in a loss of conjugation between the phenyl and naphthyl parts. The other effect is the deviation from planarity of the naphthyl and phenyl parts themselves (angles α and γ). Angle α is most sensitive to an increase in strain. It reflects the direct influence of the growing size of the *ortho* substituent. The small increase in α in the series **1c** → **1d** → **1e** hints at the possibility of the ethyl and isopropyl groups to minimize steric constraint by directing a benzylic hydrogen, not a methyl group towards the naphthalene part. This option to escape such a steric confrontation is not available to the *t*Bu substituent, thus explaining the sharp increase in α from **1e** to **f**. By contrast, the angle β,

Table 2. Deformation energies for ground (twist boat, TB) and transition states (^1T) of the lactones. ΔH_{def} (kcal/mol), $\Delta\Delta H_{def}$ referring to the difference in strain between the corresponding ground and transition states.

Stat.		Naphthyl Part		Phenyl Part		Pyranone Part	
Point	Method	ΔH_{def}	$\Delta\Delta H_{def}$	ΔH_{def}	$\Delta\Delta H_{def}$	ΔH_{def}	$\Delta\Delta H_{def}$
1a TB	AM1	3.91	–	2.14	–	8.63	–
	PM3	3.50	–	1.91	–	8.04	–
1b TB	AM1	4.35	–	4.37	–	10.83	–
	PM3	4.74	–	4.39	–	11.01	–
1c TB	AM1	4.37	–	4.71	–	12.14	–
	PM3	4.69	–	5.02	–	12.52	–
1d TB	AM1	4.43	–	5.96	–	13.13	–
	PM3	4.62	–	5.75	–	12.96	–
1e TB	AM1	4.53	–	6.10	–	13.51	–
	PM3	4.64	–	6.04	–	13.32	–
1f TB	AM1	4.64	–	11.05	–	15.32	–
	PM3	4.78	–	11.90	–	16.97	–
1a ^1T	AM1	5.71	1.80	4.16	2.02	8.72	0.09
	PM3	5.19	1.69	3.63	1.72	8.60	0.56
1b ^1T	AM1	11.56	7.21	10.68	6.31	15.33	4.50
	PM3	8.72	3.98	9.64	5.25	14.28	2.47
1c ^1T	AM1	13.29	8.92	13.35	8.64	17.92	5.78
	PM3	10.46	5.77	13.08	8.06	16.58	4.06
1d ^1T	AM1	14.00	9.57	15.47	9.51	19.16	6.03
	PM3	13.19	8.57	15.67	9.92	18.83	5.87
1e ^1T	AM1	15.40	10.87	17.49	11.39	20.04	6.53
	PM3	13.48	8.84	17.95	11.91	19.38	6.06
1f ^1T	AM1	17.71	13.07	21.89	10.84	23.82	8.50
	PM3	15.89	11.11	22.24	10.34	22.65	5.68

reflecting the torsion around the biaryl axis, varies to a distinctly smaller degree. Completely unexpectedly, the angle γ, at the periphery of the naphthyl system, even decreases over the series. It seems that the principal steric burden is shifted to the central pyranone and especially to the phenyl ring, where the backbone seems to break.

In order to quantify the energetic influence of the non–planar ring systems on the overall strain, the heats of formation of the deformed rings were compared with the corresponding unconstrained naphthalenes and benzenes, respectively. This method has already been successfully applied to binaphthyl systems.[19] The results as presented Table 2 show that apparently the naphthyl moiety is subjected to the same constant strain in all compounds. By contrast, the phenyl and pyranone deformation energies increase strongly with growing size of the substituents.

Transition structures and helimerization barriers

Encouraged by the good agreement between calculated and experimental ground structures, the transition states for the helimerization process of the lactones were calculated. Initially assuming the transition structure between the two helimeric enantiomers to be completely planar, this was found to be true exclusively for the unsubstituted parent compound **1a** (Table 3). Its transition structure could be located using the "SADDLE" algorithm implemented in VAMP 4.5, which tries to approach the transition state from two geometries on either side of the barrier. An additional NS01A optimization confirmed this stationary point. However, SADDLE failed in finding transition structures for the substituted lactones **1b–f**. Therefore, the transition structures for these compounds could not be planar, but must be distinctly twisted and thus chiral. Former force field calculations on similar bridged biaryl systems have led to the same conclusion.[20]

Table 3. Transition states for the helimerization of the lactones. Heats of formation (kcal/mol), ν_{imag} (cm^{-1}), dihedral angles (deg.). $\Delta H^{\neq}$ values are zero point corrected. For definition of dihedral angles see legend of Table 1.

Cpd.	Method	ΔH_f	$\Delta H^{\neq}$	ν_{imag}	Selected Dihedral Angles			
					α ABCD	β BCDE	γ CDEF	HCDG
1a	AM1	13.46	5.14	211.4	-0.1	-0.1	0.1	-0.1
	PM3	-0.96	2.24	171.4	0.1	0.1	-0.1	0.1
1b	AM1	-51.12	12.30	85.0	28.3	16.2	-29.9	12.4
	PM3	-65.37	8.87	62.5	25.2	10.9	-26.9	8.4
1c	AM1	16.22	18.32	81.7	34.2	16.2	-35.6	12.4
	PM3	-1.71	14.62	71.1	28.5	10.1	-32.6	7.7
1d	AM1	7.59	21.01	41.1	37.7	8.3	-39.4	7.0
	PM3	-7.49	17.31	40.4	36.1	11.7	-39.5	8.6
1e	AM1	2.96	22.89	40.4	39.6	15.9	-40.4	12.3
	PM3	-14.23	20.63	34.9	38.6	12.7	-40.6	9.6
1f	AM1	10.01	25.17	24.3	46.0	-6.0	-45.6	-2.8
	PM3	-12.90	23.52	21.8	42.7	-4.4	-44.7	-1.8

As SADDLE follows only the shortest reaction path between the two minimum structures, we now had to take into account more complex movements describing the interconversion of the enantiomeric structures. In order to systematically search for all conceivable geometries that could be of significance for transition structures, we made use of grid calculations. Careful examinations showed that a variation of the two dihedral angles FEDB and ABDE results in steady potential surfaces with four stationary points, two of which resemble the two enantiomeric ground states. The other two stationary points were found to be saddle points. Their geometries were used as input geometries for NS01A calculations, which revealed these points to be very close to the actual transition states. Force calculations confirmed all NS01A results, as only one imaginary eigenvalue was found. To ensure that the transition states represent the ones corresponding to the helimerization process, intrinsic reaction coordinate (IRC) calculations were performed. In every case these calculations led to the previously determined global minima.

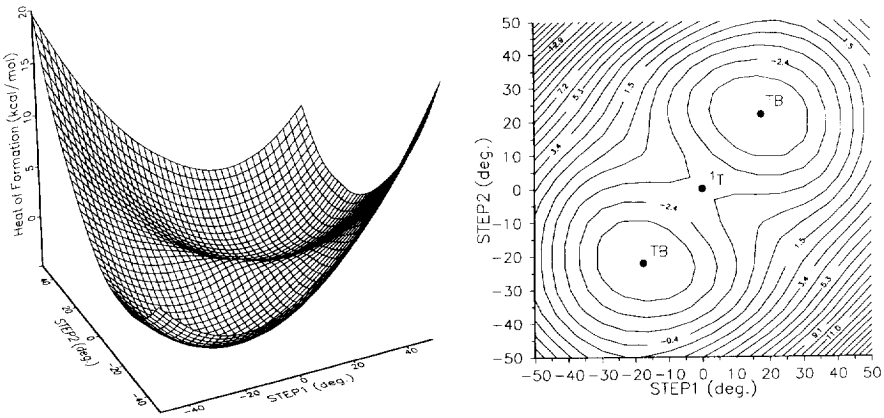

Fig. 2. 3D view and contour plot of the potential surface for the helimerization process of **1a** (PM3). STEP 1 (dihedral angle FEDB), STEP 2 (dihedral angle BCDE). Dihedral angles refer to the legend of Table 1.

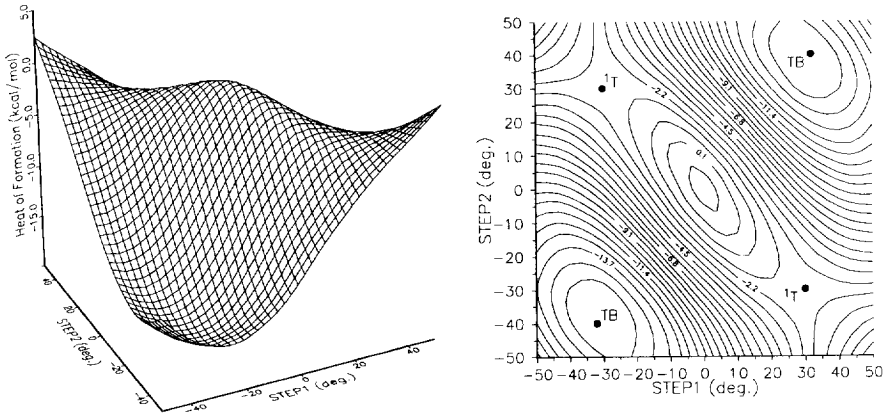

Fig. 3. 3D view and contour plot of the potential surface for the helimerization process of **1c** (PM3). STEP 1 (dihedral angle FEDB), STEP 2 (dihedral angle ABDE). Dihedral angles refer to the legend of Table 1.

A comparison of the IRC reaction path with the steepest–descend–path on the potential surface reveals a striking resemblance. Thus it can be concluded that the two dihedral angles FEDB and ABDE as driving angles for the grid calculations are well suited to describe the isomerization process. In order to exclude other reaction paths for compound **1a**, we searched for a method to describe its potential surface as well. Best results were obtained with angles FEDB and BCDE. The potential surface shows the planar structure to be the only saddle point, it directly connects the two minima. Figures 2 and 3 show 3D views and contour plots of the grids for compound **1a** and **1c**. The isomerization process that we describe here can be classified as a "narcissistic" reaction.[21] For such reactions there exist just the two reaction paths that we found here within the same class of compounds: a passage "through the mirror" with a transition state of higher symmetry (**1a**, Figure 2) and a passage "around the mirror"[21] with two enantiomeric transition states (all others **1b–f**, Figure 3). The latter path implies a non–synchronous movement of the molecule. In either direction to a transition state, almost exclusively one moiety (phenyl/naphthyl) is bent away from the other.

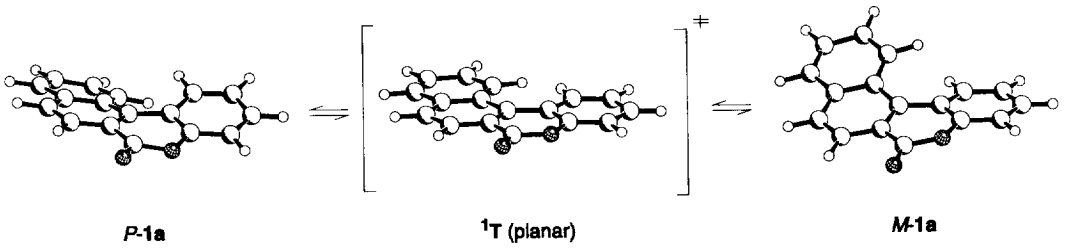

Fig. 4. Enantiomeric ground structures (*M*–**1a**, *P*–**1a**) and planar transition structure (^{1}**T**) on the reaction pass of the helimerization process of **1a**

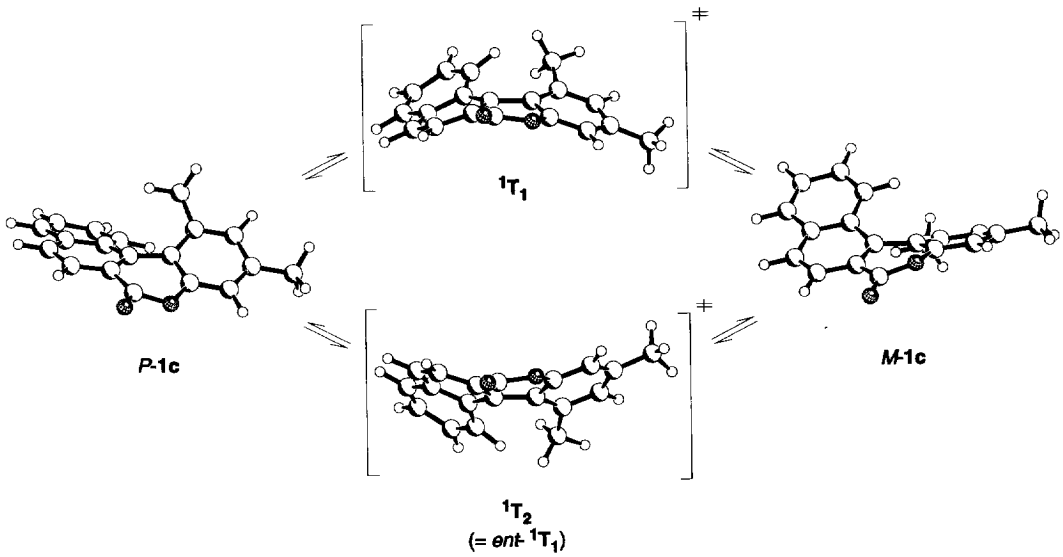

Fig. 5. Enantiomeric ground (*M*–**1c**, *P*–**1c**) and transition structures (^{1}**T**$_1$, ^{1}**T**$_2$) on the reaction pass of the helimerization process of **1c**

Table 2 summarizes selected properties of the transition states including the activation enthalpy $\Delta H^{\neq}$ for the helimerization process. As expected, the activation energy increases with increasing size of substituents. There is a marked difference between PM3 and AM1 results, the latter being 3 to 4 kcal/mol higher.[22] This might in part be attributed to the fact that the endocyclic C–O bond length is ca 0.1 Å shorter in the PM3 structures than those in AM1, resulting in a relief of strain between naphthyl–H and the ortho substituent and more planar transition structures. Indeed, the PM3 transition structures are more planar, as can be seen from the dihedral angle values in Table 3. Thus, the PM3 reaction path describes a smaller loop "around the mirror" than AM1. Figures 4 and 5 show ball–and–stick plots of the stationary points through the reaction pass of the helimerization of **1a** and **1c**. The increasing distortion of the geometries for both ground and transition structures is obvious, ground structures forming a helix, transition structures forming an arc. Deformation energies for transition structures and their differences to the corresponding ground structure energies (Table 3) show an overall increase in deformation for every ring system in itself. Phenyl and naphthyl parts seem to be more sensitive towards an increase in substituent size. There is a good correlation between the activation barriers and the overall deformation energies, which suggests that ring deformation plays a major role in the barrier. It should however be noted that the sum of the deformation energies cannot equal the activation energy, because part of the strain would thus be regarded twice due to the "overlap" of the three ring systems. In addition, conjugational and steric repulsion effects might be important for the size of the activation barrier.

In order to verify our results obtained by semiempirical calculations which are known to produce rotational barriers that are too low compared with the experiment, *ab initio* calculations were carried out. Unfortunately, the higher level *ab initio* methods (RHF/3–21G, MP2/6–31G*) used here require a large number of basis functions for these fairly large lactone systems, so that the computational expenditure is very high. Therefore *ab initio* calculations were performed exclusively for compound **1c**, which represents an intermediate case concerning the steric demand of the *ortho* substituents.

While the *ab initio* calculated ground structure matches very well with that obtained by semiempirical methods, as can be seen from the RMS values in Table 4, the transition structure is more planar (see the values for the corresponding dihedral angles in Table 4), but still significantly concave in shape. With regard to this fact it is surprising that the values for the activation enthalpies (Table 4) are actually higher than those predicted by the semiempirical methods, especially those obtained from the PM3 calculations.

Table 4. Ground and transition structures for the helimerization of the lactone **1c**. Heats of formation (kcal/mol), ν_{imag} (cm^{-1}), dihedral angles (deg.), total energies E_{tot} (Hartree). $\Delta H^{\neq}$ values are zero point corrected. Geometries were calculated with RHF/3–21G; energies exclusively were calculated with MP2/6–31G* on the RHF/3–21G stuctures.

Stat.					α	β	γ		RMS	
Point	Method	E_{tot}	$\Delta H^{\neq}$	ν_{imag}	ABCD	BCDE	CDEF	HCDG	AM1	PM3
TB	SCF/3–21G	-872.5156	–	–	13.4	32.9	16.5	34.1	0.047	0.054
TB	MP2/6–31G*	-880.1735	–	–	–	–	–	–	–	–
^{1}T	SCF/3–21G	-872.4813	22.28	80.76	14.4	4.7	13.9	4.0	0.338	0.275
^{1}T	MP2/6–31G*	-880.1397	21.93	–	–	–	–	–	–	–

SUMMARY

Summarizing, semiempirical and *ab initio* calculations reveal that the six substituted benzo[b]naphtho-[1,2–d]pyranones show an interesting isomerization behaviour. While compound **1a** passes through a transition geometry in which the ring system is completely planar, all the others possess two enantiomeric transition structures. The helimerization barrier increases with the size of the *ortho* substituent and can be well correlated to an increase in deformation energy of the isolated ring systems. Semiempirical as well as *ab inito* geometries of the ground states match very precisely with X–ray structures. The *ab initio* transition structure of **1c** has a similar shape as the semiempirical one, but is more planar. *Ab initio* and AM1 activation energies agree well, whereas the PM3 barrier seems to be too small.

ACKNOWLEDGEMENTS

We gratefully acknowledge financial support from the Deutsche Forschungsgemeinschaft (Sonderforschungsbereich No. 347 "Selektive Reaktionen Metall–aktivierter Moleküle", project B–1) as well as the Fonds der Chemischen Industrie. We also wish to thank Dr. T. Clark for fruitful discussions and K.–P. Gulden for valuable technical support.

REFERENCES

1. "Novel Concepts in Directed Biaryl Synthesis", part 52; for part 51, see ref. 5.
2. Bringmann, G.; Walter, R.; Weirich, R. *Angew. Chem.* **1990**, *102*, 1006–1019; *Angew. Chem. Int. Ed. Engl.* **1990**, *29*, 977–991.
3. Bringmann, G.; Göbel, L.; Schupp, O. *GIT Fachz. Lab.* **1993**, 189–200.
4. Bringmann, G. *South African J. Chem.* **1995**, in press.
5. Bringmann, G.; Harmsen, S.; Schupp, O.; Walter, R. Metall Assisted "Twisting" of Axes: A Novel Approach to Stereoselective Biaryl Synthesis. In *Selective Reactions of Metal–Activated Molecules*; Werner, H.; Sundermeyer, J. Eds.; Vieweg: Braunschweig, 1995, in press.
6. Bringmann, G.; Hartung, T.; Göbel, L.; Schupp, O.; Ewers, Ch. L. J.; Schöner, B.; Zagst, R.; Peters, K.; von Schnering, H. G.; Burschka, Ch. *Liebigs Ann. Chem.* **1992**, 225–232.
7. Bringmann, G.; Schöner, B.; Schupp, O.; Peters, E–M.; von Schnering, H.G. *Liebigs Ann. Chem.* **1994**, 91–97.
8. Bringmann, G.; Hartung, T. *Tetrahedron* **1993**, *49*, 7891–7902.
9. Dewar, M. J. S.; Zowebisch, E. G.; Healy, E. F.; Stewart, J. J. P. *J. Am. Chem. Soc.* **1985**, *107*, 3902.
10. Stewart, J. J. P. *J. Comput. Chem.* **1989**, *10*, 209–220.

11. VAMP 4.5 (vectorized version of a MO program on the basis of AMPAC and MOPAC): Rauhut, G.; Chandrasekhar, J.; Clark, T. University of Erlangen–Nürnberg, 1992.

12. SYBYL: Tripos Associates, 1699 St. Hanley Road, Suite 303, St. Louis, MO, 63144.

13. Powell, M. J. D. *Nonlinear Optimization*, Academic Press: New York, 1982.

14. Trucks, G. W.; Head–Gordon, M.; Gill, P. M. W.; Wong, M. W.; Foresman, J. B.; Johnson, B. G.; Schlegel, H. B.; Robb, M. A.; Replogle, E. S.; Gomperts, R.; Andres, J. L.; Raghavachari, K.; Binkley, J. S.; Gonzalez, C.; Martin, R. L.; Fox, D. J.; Defrees, D. J.; Baker, J.; Stewart, J. J. P.; Pople, J. A. Gaussian, Inc., Pittsburgh PA, 1992.

15. Baker, J. *J. Comput. Chem.* **1987**, *8*, 563–571.

16. Peters, K.; Peters, E.–M.; von Schnering, H. G.; Bringmann, G.; Hartung, T.; Schupp, O. *Z. Kristallogr.* **1992**, *202*, 271–274.

17. Peters, K.; Peters, E.–M.; von Schnering, H. G.; Bringmann, G.; Hartung, T. *Z. Kristallogr.* **1992**, *202*, 275–278.

18. Bringmann, G.; Dauer, U.; Schupp, O.; Lankers, M.; Popp, J.; Posset, U.; Weippert, A.; Kiefer, W. *Inorg. Chim. Acta* **1994**, *222*, 247–253.

19. Kranz, M.; Clark, T.; von Ragué–Schleyer, P. *J. Org. Chem.* **1993**, *58*, 3317–3325.

20. Müllen, K.; Heinz, W.; Klärner, F.–G.; Roth, W.R.; Kindermann, I.; Adamczak, O.; Wette, M.; Lex, J. *Chem. Ber.* **1990**, *123*, 2349–2371.

21. Salem, L. *Acc. Chem. Res.* **1971**, *4*, 322–328.

22. Fabian, W. M. F. *J. Comput. Chem.* **1988**, *9*, 369–377.

(*Received in Germany* 25 *November* 1994; *accepted* 26 *January* 1995)